



Egyptian Journal of Agricultural Research

Plant Pathology

Green synthesis of zinc oxide nanoparticles from *Schefflera* arboricola extract to enhance onion resistance to downy mildew, promote growth, and contribute to sustainability

Sozan E. El-Abeid¹; Heba Yousef¹; Ahmed M. Saleh²; Eman Y. Khafagi*¹

Address:

- ¹ Plant Pathology Research Institute, Agricultural Research Center, Giza, Egypt
- ² Department of Pharmaceutical Chemistry, Faculty of Pharmacy, Horus University, Egypt.
- *Corresponding author: *Eman Khafagi.* email: <u>dr_emankhafagi@yahoo.com</u>

Received: 12-10-2025; **Accepted:** 01-11-2025; **Published:** 05-11-2025 **DOI:** 10.21608/EJAR.2025.431879.1747

ABSTRACT

This research focused on the green synthesis of zinc oxide nanoparticles (ZnO-Sca-NPs) using *Schefflera* arboricola extract and evaluated their efficacy against onion downy mildew (*Peronospora destructor*). GC-MS analysis of the plant extract revealed caffeic acid (80.69%) as the major compound, indicating strong antioxidant potential. SEM, TEM, XRD, and FTIR analyses confirmed spherical nanoparticles (<80 nm) with a crystalline hexagonal structure and ZnO bonds, validating their successful synthesis. Field experiments showed dosedependent reductions in disease severity, with 100 mg/L ZnO-Sca-NPs achieving 11.24 and 13.54% severity and 82.29 and 76.26% efficacy across two seasons, along with improved bulb yield and phenolic content. SDS-PAGE analysis revealed the induction of a ~48 kDa protein band, suggesting activation of plant defense proteins. Cytotoxicity testing of ZnO-Sca-NPs on primary human uterine fibroblast cells indicated acceptable biocompatibility at ≤50 mg/L. Overall, ZnO-Sca-NPs demonstrated effective antifungal activity, growth promotion, and defense activation, supporting their viability as eco-compatible replacements for traditional fungicides.

Keywords: Zinc nanoparticles; *green synthesis*; *Peronospora destructor*; Antifungal activity; Plant defense.

INTRODUCTION

Among vegetable crops, *Allium cepa* L. (Onion) is a vital crop globally and especially in Egypt, where it plays a major role in agricultural production and exports. Egypt ranks among the top producers in the MENA region, with key cultivation areas such as Beni Suef, Minya, Fayoum, and Kafr El-Sheikh (FAO, 2023; Ministry of Agriculture and Land Reclamation, 2023; Agricultural Economics Research Institute, 2023). As a valuable export commodity, the onion plant ranks fourth among Egypt's vegetable and fruit exports, with over 816,000 tons exported in 2023, valued at approximately \$145.8 million (Abd El-Fattah *et al.*, 2024). Beyond its economic importance, the onion is a dietary staple in Egyptian households and is valued for its health-promoting effects due to its rich composition of bioactive molecules exhibiting antioxidant, anti-inflammatory, and anti-carcinogenic properties (Amar *et al.*, 2025). It has extensive applications in the food processing and preservation sectors and in traditional medicine, aiding in digestive and respiratory conditions, cancer prevention, and thrombosis (Nicastro *et al.*, 2015). Moreover, its industrial uses in the pickling and drying sectors contribute to income and employment (Amr *et al.*, 2019).

Despite significant economic and nutritional importance, onion (*A. cepa*) production in Egypt is frequently threatened by the oomycete pathogen *Peronospora destructor*, the causal agent of onion downy mildew. This pathogen is recognized of the most destructive worldwide (Koike *et al.*, 2007). *P. destructor* is an obligate biotrophic oomycete that primarily infects the foliage, inducing chlorosis, leaf curling, and necrosis, which collectively result in considerable yield losses and deterioration of bulb quality (Schwartz & Mohan, 2008). The disease develops optimally under cool and humid conditions, with maximum sporulation occurring between 10–15°C and relative humidity exceeding 90% (Galván *et al.*, 2008). Airborne sporangia promote rapid disease dissemination within and among fields, often leading to severe economic losses, particularly in regions characterized by intensive onion cultivation (Thomas *et al.*, 2014).

In Egypt, the disease has become increasingly prevalent since 2016, posing a serious threat to local production and export potential (Ministry of Agriculture and Land Reclamation, 2022). Current management

strategies rely heavily on fungicidal applications and cultural practices; however, the emergence of fungicide-resistant strains and environmental concerns has highlighted the need for safer and more sustainable alternatives (Ahmed *et al.*, 2021). Recently, biological and nanotechnology-based methods such as the green synthesis of zinc oxide nanoparticles have received increasing attention as promising eco-friendly approaches to control fungal infections (El-Abeid *et al.*, 2024a; Sangeeta *et al.*, 2024).

Zinc (Zn) is an essential micronutrient vital for plant growth, soil fertility, and human health; however, Zn deficiency limits crop productivity and food quality (Sethi *et al.*, 2025). Zinc oxide (ZnO) exhibits notable antimicrobial activity, but conventional ZnO particles suffer from low solubility and reactivity (Raghupathi *et al.*, 2011; Sirelkhatim *et al.*, 2015). In contrast, zinc oxide nanoparticles (ZnO-NPs) possess nanoscale dimensions, large surface area, and high bioactivity, enabling the generation of reactive oxygen species (ROS) that disrupt microbial membranes and DNA, thereby enhancing antifungal efficacy against pathogens such as *Peronospora destructor* (Singh *et al.*, 2018; Raha and Ahmaruzzaman *et al.*, 2022).

Plants rich in polyphenols and flavonoids provide natural reducing and stabilizing agents for the green synthesis of ZnO-NPs, influencing particle morphology and bioactivity (Choi *et al.*, 2017; Drishya *et al.*, 2025). Green-synthesized ZnO-NPs thus offer sustainable, eco-friendly alternatives to chemical fungicides, improving plant vigor and soil health (Choudhary *et al.*, 2023; El-Abeid *et al.*, 2024a).

Schefflera arboricola, rich in bioactive compounds, has shown promise in nanoparticle biosynthesis, supporting its application in sustainable plant disease management and nanomedicine (Choudhary et al., 2023). Furthermore, toxicity assessment on human cells has confirmed the biosafety of ZnO-Sca-NPs, highlighting their potential as a safe, green alternative for sustainable crop protection and human health (Anjum et al., 2021).

Given this background, the use of plant-derived polyphenols in the green synthesis of metal oxide nanoparticles—particularly ZnONPs—holds significant promise for developing environmentally benign and biologically active nanomaterials capable of controlling plant pathogens and alleviating oxidative stress (Swain et al., 2025).

This study presents zinc oxide nanoparticles (ZnO-Sca-NPs) that were biosynthesized using *S. arboricola* (Sca) leaf extract for the first time. Which is rich in bioactive components, was identified via GC-MS analysis. Additionally, a simple surface functionalization approach was applied to examine ZnO nanoparticles with antioxidant compounds from Sca. This study aims to synthesize zinc oxide nanoparticles (ZnO-NPs) using *S. arboricola* leaf extract through an environmentally friendly green synthesis approach. The synthesized nanoparticles were characterized both physically and chemically to confirm their formation and stability, while the bioactive components of the plant extract were identified using GC-MS analysis. The antifungal efficacy of the biosynthesized ZnO-NPs was evaluated in vivo against *P. destructor*, the causal agent of onion downy mildew, and their performance was compared with that of conventional ZnO formulations. In addition, cytotoxicity assessments on human cell lines were conducted to ensure biosafety and environmental compatibility. Overall, this research proposes a sustainable and effective strategy for crop protection that integrates nanotechnology with plant-derived bioresources, contributing to the development of green alternatives to traditional fungicides.

MATERIALS AND METHODS

Materials:

Zinc acetate dihydrate (Zn (CH3COO) 2·2H2O, 99.0%) and Zinc bulk (ZnO) were obtained from LOBA Chemie. Fungicide Amistar top (SC) 32.5% (Azoxystrobin + Difenoconazole), Shoura, Syngenta Agro. Egypt. All chemicals were used as received without further purification. Deionized water was used throughout the experiments. *S. arboricola* plant (Sca) was prepared from fresh leaves of the plant collected from the Agriculture Research Center garden.

Methods:

- GC-MS analysis of the S. arboricola extract:

Gas chromatography-mass spectrometry (GC-MS) analysis was performed to identify the main bioactive compounds in *S. arboricola* (Sca) leaf extracts, aiming to identify the components likely responsible for promoting the synthesis of zinc nanoparticles with higher efficacy. GC-MS profiling of *S. arboricola* leaf extracts was conducted utilizing a model Agilent 7890B GC device in conjunction with a 5977A mass selective detector (Agilent Technologies, USA) at the central laboratories network of the National Research Center, Egypt. The chromatographic separation was performed on a DB-5MS capillary column (30 m \times 0.25 mm internal diameter, 0.25 μ m film thickness). Hydrogen served as the carrier gas and was maintained at a constant flow rate of 1.0 mL min⁻¹ in splitless injection mode, with an injection volume of 1 μ L. The oven temperature program was initiated at 60 °C

for 1 min, then increased at a rate of 10 °C min⁻¹ up to 320 °C, and held for an additional 10 min. Injector and detector temperatures were set at 300 °C and 320 °C, respectively. Mass spectra were recorded under electron ionization (EI, 70 eV) over an m/z range of 50–800, with a solvent delay of 7.3 min. The ion source and quadrupole temperatures were maintained at 230 °C and 150 °C, respectively.

Identification of individual compounds was achieved by comparing the obtained mass fragmentation patterns with those in the NIST and Wiley spectral databases.

- Biosynthesis of Zinc oxide nanoparticles (ZnO-Sca-NPs):

Biosynthesis of ZnO–Sca NPs Zinc oxide nanoparticles (ZnO-Sca-NPs) were synthesized via a green method using *S. arboricola* (Sca) extract as a reducing and stabilizing agent. The (Sca) extract was prepared by heating 30 g of fresh leaves in 100 mL of deionized water at 70 °C with continuous stirring at 1000 rpm for 30 min. The extract was then filtered through filter paper (No.1). Next, 10 mL of 0.1 M zinc acetate dihydrate solution was added to 90 mL of Sca under stirring at 1000 rpm. The pH was adjusted to 8 by adding NH₄OH solution. A white precipitate of ZnO-Sca-NPs was immediately formed. The precipitate was centrifuged at 5000 rpm for 15 min and washed twice with deionized water. Finally, the ZnO NPs were then dried at 100 °C for 2 h to obtain ZnO-Sca-NPs powder. For subsequent biological and field experiments, a stock solution was prepared by dispersing the ZnONPs powder in distilled water at concentrations of 25, 50, 75, and 100 mg/L. The dispersion was achieved using ultrasonication for 30 min to ensure homogeneity and prevent agglomeration, according to (Sagar and Thorat, 2015).

• Characterization and microscopic analysis:

Nanoparticles' morphology and size were characterized by Transmission electron microscopy (TEM) (TEM, Philips, Amsterdam, Netherlands) and Scanning electron microscopy (JEOL Company, voltage of 300 kV, Japan). Crystalline structure and composition were determined by X-ray diffraction (XRD) (Brucker D2 phaser 2nd Gen German). Additionally, the NPs were analyzed with FT-IR spectrum (4000:400 cm-1) using a Nicolet iS50 FTIR Thermo spectrometer.

• Field Experimentation:

Field experiments were conducted over two consecutive growing seasons in 2022-2023 and 2023-2024 in a field naturally infested with *P. destructor*, the causal agent of downy mildew. The trials were carried out in the Qalyubia Governorate, Egypt. A randomized complete block design (RCBD) with four replicates was used. Each experimental plot measured 3.0 × 3.5 m (10.5 m²), equivalent to 1/400 feddan, and consisted of six rows. Sixty-day-old transplants of onion (*Allium cepa* L.), cultivar Giza 20, were transplanted into each plot at a spacing of 10 × 10 cm within and between rows during the first week of December. All recommended agronomic practices for onion cultivation were applied throughout the growing period. The effectiveness of T1: Zinc oxide nanoparticles (ZnO-Sca-NPs) at a concentration of 25mg/L, T2: ZnO-Sca-NPs at 50 mg/L, T3: ZnO-Sca-NPs at 75 mg/L, T4: ZnO-Sca-NPs at 100 mg/L was investigated, in comparison with zinc bulk (ZnO) at 2000 mg/L (Subbaiah *et al.*, 2016) and fungicide Amistar top (SC) 32.5% (Azoxystrobin + Difenoconazole) that was applied at the recommended rate 300 cm / feddan (400 L water) as foliar spray, 40 days after transplanting for four times at 15-day intervals.

- Disease and yield assessment:

a) Disease severity of downy mildew was recorded after three months trans (at the first week of March). One hundred leaves from each plot were chosen as randomized samples to determine disease severity the studied disease, and were monitored using a (0-8) scale and recorded according to the method described by (Townsend and Heuberger, 1943) as follows:

0 = no infection (leaves are completely healthy), 1= 1-2 spots per onion leaf, 2 = 3-5 spots per onion leaf, 3 = 6-10 spots per onion leaf, 4= 25% of leaf surface was attacked, 5= 35 - <50% of leaf surface was attacked, 6= 50% of leaf surface was attacked, 7= 75% of leaf surface was attacked, 8 more than 75% of leaf surface was attacked. Disease severity index of downy mildew was estimated using the following formula:

D.S.I=
$$\frac{\Sigma (n \times v)}{ZN} \times 100$$

Where:

D.S.I = Disease severity index, n = Number of leaves in each category, v = Numerical value of each category, Z = Numerical value of the highest category, and N = Total number of leaves in the sample.

b) Onion bulb yield as kg/plot (10.5 m²) was weighted in all treatments after harvesting.

- c) Percentages of treatment efficacy in reducing the disease infection were calculated as follows: % Treatment efficiency = ((Control-treatment)/Control) X 100. (Mahmoud *et al.*, 2016)
- Effect of zinc treatments on biochemical changes:

• Determination of phenolic contents:

The concentrations of free, conjugated, and total phenols were determined according to the method described by (Zieslin and Ben-Zaken, 1993), with slight modifications. Samples of leaves of onion plant (1g) were taken after two days from the second foliar sprays and extracted for phenolic compounds according to Zieslin and Ben-Zaken (1993). One milliliter of the sample extract was mixed with 0.25 mL of hydrochloric acid (HCl) and heated in a water bath at 100 °C for 10 minutes, followed by cooling to room temperature. Subsequently, 1 mL of Folin–Ciocalteu's reagent and 6 mL of sodium carbonate (Na₂CO₃) solution were added to the mixture. The final volume was then adjusted to 10 mL with distilled water. The optical density of the resulting solution was measured using a spectrophotometer at 520 nm. Phenolic content was expressed as milligrams per gram of fresh weight per minute (mg/g FW/min).

• SDS-PAGE analysis:

Proteins were extracted from onion tissues using the method of (Guseva and Gromova, 1982). The samples of leaves of the onion plant (5g) were taken after two days from the second foliar sprays and ground into a fine powder using liquid nitrogen. The resulting powder was then suspended in phosphate buffer (pH 8.3) at a ratio of 1–3 mL buffer per gram of tissue. Extracts were centrifuged, and protein concentration was determined by the Bradford assay (Bradford, 1976) using BSA as a standard. Protein profiles were separated by SDS-PAGE according to (Laemmli, 1970) and visualized by silver nitrate staining (Sammons *et al.*, 1981). Banding patterns were analyzed using a gel documentation system, and cluster analysis was performed by the UPGMA method (Sneath and Sokal, 1973).

• Cytotoxic activity test:

The sample was tested against a normal human cell line using the MTT assay. Seed cells in a 96-well plate.50 μ L of serum-free medium and 50 μ L of MTT solution were added to each well. Incubate the plate at 37°C for 3 hours. After incubation, 150 μ L of MTT solvent was added to each well. The plate was wrapped in aluminum foil and shaken on an orbital shaker for 15 minutes. The viable cells contain NAD (P)H-dependent oxidoreductase enzymes, which reduce the MTT to formazan, which is insoluble. The formazan crystals are then dissolved using a solubilization solution, and the resulting colored solution is quantified by measuring absorbance at 570 nanometers using a multi-well spectrophotometer (Terpiłowska *et al.*, 2018). And viability is calculated as follows: Viability % = 100 x OD570t/OD570c.

OD570t = Optical density absorbance at 570 of treatment; and OD570c = Optical density absorbance at 570 of control. The IC50 was estimated using both the IC $_{50}$ calculator and GraphPad programs (Sánchez-Díez et al., 2025).

Statistical analysis:

Statistical analysis was performed using SPSS software (version 23.0; IBM Corp., Chicago, IL, USA) through a one-way analysis of variance (ANOVA). Duncan's multiple range test was employed to assess significant differences among the treatment means of P<0.05(Chinnasami and Manickam, 2023).

RESULTS

• GC-MS analysis of the S.arboricola extract:

GC-MS analysis of the *S. arboricola* extract (Table 1 and Fig. 1) led to the identification of thirteen major phytochemical constituents, primarily in the form of their trimethylsilyl (TMS) derivatives. Among these, caffeic acid (3TMS derivative) was the most dominant compound, exhibiting a retention time (RT) of 16.041 min and comprising 76.07% of the total chromatographic peak area. Caffeic acid is a well-known hydroxycinnamic acid with established antioxidant and anti-inflammatory properties, and its high abundance suggests a central role in the biological activity of the extract. In addition to caffeic acid, other prominent metabolites included malic acid (11.41%), 4-coumaric acid (6.27%), and arabino furanose (3.48%), detected at retention times of 9.422, 14.078, and 12.266 min, respectively. Malic acid is involved in primary metabolism and abiotic stress response, while coumaric acid and arabino furanose are linked to secondary metabolic pathways and cell wall structure. Minor constituents such as ferulic acid, citric acid, palmitic acid, alpha-linolenic acid, and sebacic acid were also identified, each contributing less than 1 % of the total peak area. These compounds, although present in smaller quantities, may contribute to synergistic bioactivities related to plant defense, lipid metabolism, and antioxidant potential.

The overall chemical profile of the extract indicates a metabolically rich composition dominated by phenolic acids

Table 1. Integration peak list of the total ion chromatogram (TIC) of S. arboricola extract detected by GC-MS.

	Table 1. Integration peak list of the total ion chromatogram (TIC) of <i>S. arboricola</i> extract detected by GC-MS.					
Peak	RT	Height	Area %	Spectrum structure	Spectrum structure shape	
1	9.422	16289813	11.41	Malic acid, 3TMS derivative	013	
2	10.815	133342	0.1	2,3-Dihydroxy-3- methylpentanoic acid, 2TMS	HOC HOC OH	
3	12.266	5028199	3.48	Arabinofuranose, 1,2,3,5-tetrakis-O- (trimethylsilyl)	113C 013	
4	13.063	70561.7	0.08	Citric acid, 4TMS derivative	H3C OH3 OH3 OH3	
5	14.078	8585736	6.27	4-Coumaric acid, 2TMS	H3C OH3 OH3 OH3	
6	15.018	1489829	1.03	Palmitic Acid, TMS derivative	H3C 5 0H3 0H3	
7	15.521	52138.15	0.09	Ferulic acid, 2TMS derivative	H3C 0-13 0-13 0-13 0-13 0-13 0-13 0-13 0-13	
8	16.041	60852264	76.07	Caffeic acid, 3TMS derivative	H3C OH3 OH3	
9	16.67	304626.8	0.46	alphaLinolenic acid, TMS derivative	H3C CH3	
10	16.897	70360.96	0.06	Stearic acid, TMS derivative	H3C 5 CH3 CH3	
11	19.556	104619.5	0.16	Sebacic acid, 2TMS derivative	H3C CH3 OH3 OH3	
12	21.871	128758.3	0.62	2- Trimethylsilyloxysebacic acid, bis(trimethylsilyl)- ester	H3C CH3 CH3 CH3 CH3 CH3 CH3 CH3 CH3 CH3	
13	22.92	16751.8	0.07	o-Coumaric acid, 2TMS derivative	0-13 0-13 0-13	

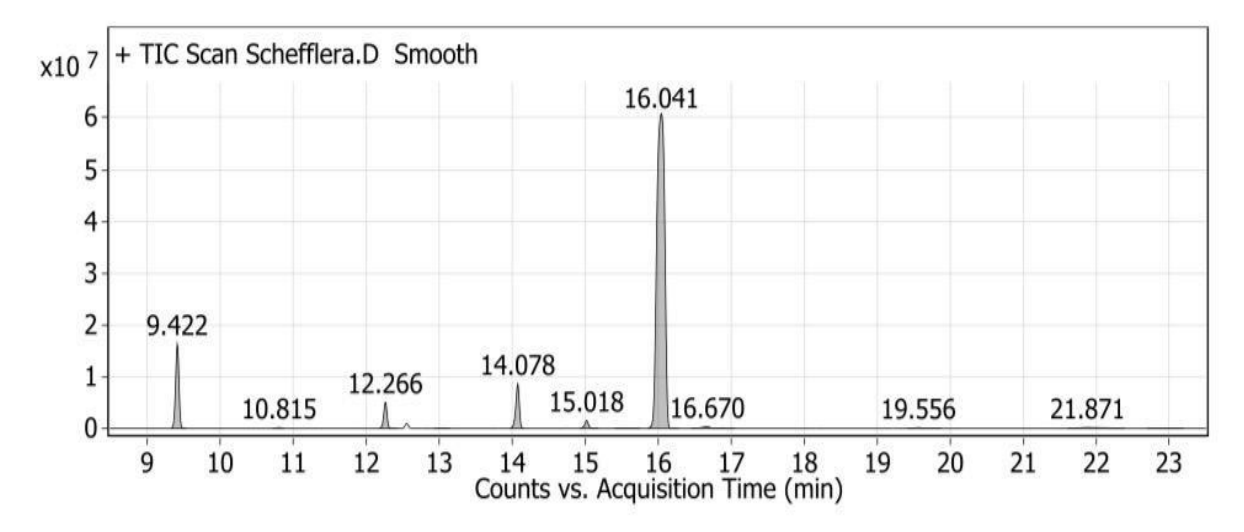


Fig. 1. Total ion chromatogram (TIC) of S. arboricola extract detected by GC-MS

and organic acids, with potential relevance to pharmaceutical, nutraceutical, and plant stress physiology applications. The presence of several bioactive compounds supports the potential use of Schefflera extracts in plant-based biotechnology and functional product development.

• Nanoparticles preparation and characterization:

The biosynthesis of zinc oxide nanoparticles (ZnO-Sca-NPs) using *S. arboricola* (Sca) leaf extracts showed significant efficacy, resulting in well-dispersed and substantially uniform nanoparticles. Subsequent to thermal drying at 100 °C for 2 hours, the obtained ZnO-SCA-NPs white powder was subjected to morphological and structural analysis. The uniform dispersion of the nanoparticles is verified by SEM and TEM images. The findings suggest that the ZnO-Sca-NPs exhibited a spherical shape with a size distribution under 80 nm, as seen in (Fig. 2 and Fig.3B). The TEM pictures confirm the particle size and homogeneous spherical shapes, demonstrating that the plant extract (Sca) caused the observed size. The crystallinity of the nanoparticles was investigated by X-ray diffraction (XRD) (Fig. 3C). The XRD pattern of the green-synthesized ZnO-Sca-NPs displayed several diffraction peaks corresponding to the hexagonal wurtzite structure of ZnO. The diffraction peaks at 2θ values of 31.82°, 34.47°, 36.30°, 47.60°, 56.67°, 62.93°, 66.03°, 67.8°, 68.15° and 76.6° correspond to the (100), (002), (101), (102), (110), (103), (200), (112), (201), and (202) planes, respectively, confirming the high crystallinity and purity of the synthesized nanoparticles.

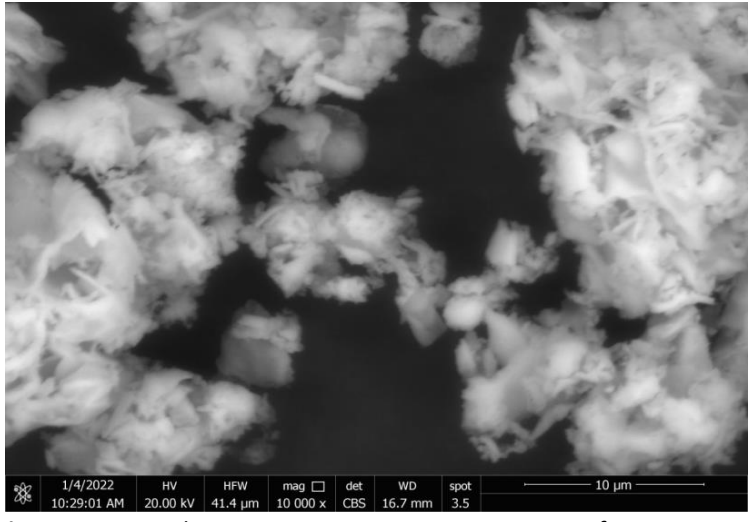


Fig. 2. Scanning electron microscopy images structure of ZnO-Sca-NPs.

Quantitative FTIR analysis was performed to identify the functional group present in the case of ZnO-Sca-NPs, as shown in (Fig. 3A). The absorption spectrum of the sample exhibited a sharp band below 600 cm⁻¹, which is attributed to the stretching vibration of the Zn–O bond. Additionally, a broad peak observed at 3320 cm⁻¹ is associated with the O–H bond vibrations of alcohol groups. Furthermore, the absorption band centered at 1567 cm⁻¹ corresponds to C=C stretching vibrations of aromatic rings. Whereas the peak at 1396 cm⁻¹ is associated with O–H bending in carboxylic acid groups, while the band near 1337 cm⁻¹ likely arises from O–H bending vibrations in alcohol groups. Finally, these regions indicate major absorption peaks at 1567–1337 cm⁻¹, which correspond to asymmetric and symmetric stretching modes of the carboxylate group. Peaks at 1017 cm⁻¹ (C–F stretching), 828 cm⁻¹ (aromatic C=C bending), 676 cm⁻¹ (C–Cl stretching), and additional absorptions at 614, 512, 490, 479, and 439 cm⁻¹ were also detected, corresponding to O–H stretching, CO₂ modes, and C=O stretching vibrations, respectively. A broad absorption peak indicative of the O–Zn–O group's vibration was noted in the range of 676–400 cm⁻¹, particularly at 512.68 and 455.76 cm⁻¹.

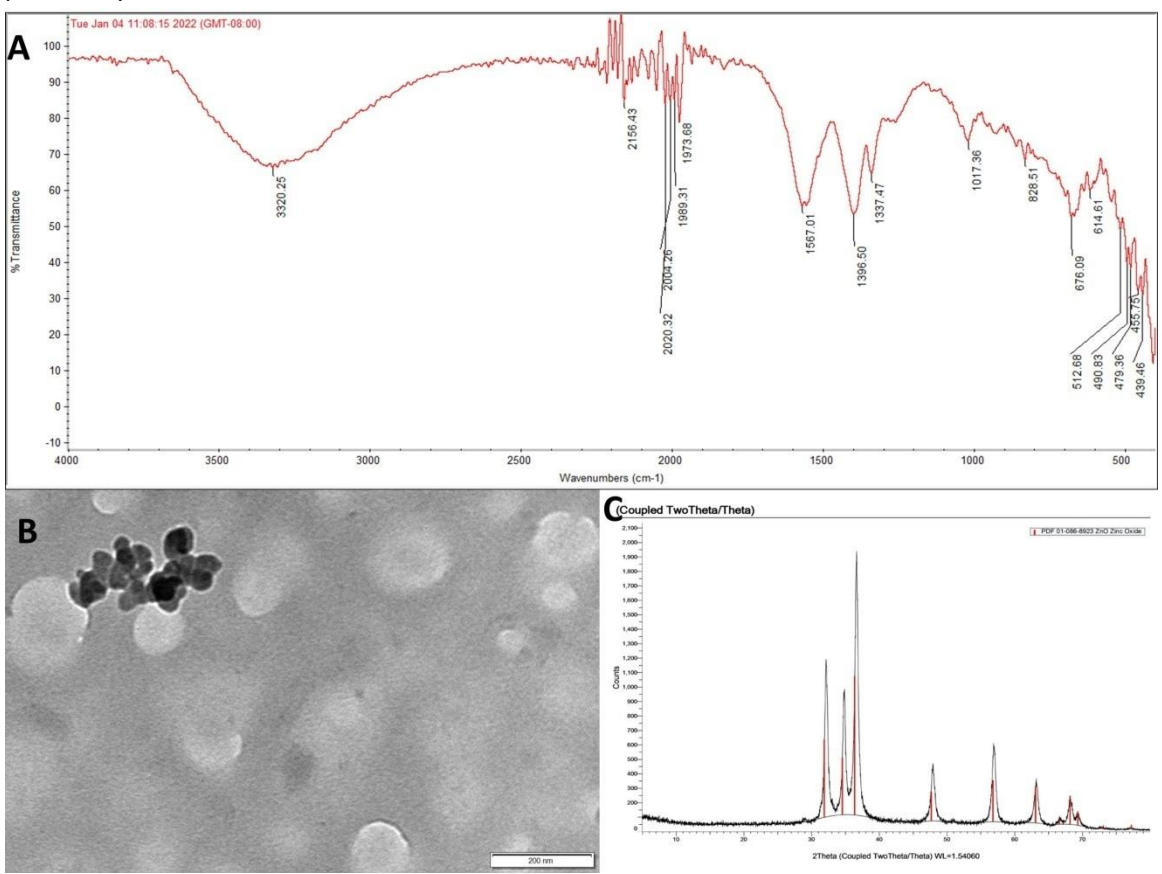


Fig. 3. FTIR analysis of FTIR of ZnO-Sca-NPs (A); Transmission electron microscopy images of structures of ZnO-Sca-NPs (B), XRD of ZnO-Sca-NPs (C).

• Effect of zinc treatments on disease severity of onion downy mildew and bulb yield:

A two-season field experiment was conducted to evaluate the impact of biosynthesized zinc oxide nanoparticles (ZnO-Sca-NPs) and their bulk counterpart zinc (ZnO) on the downy mildew fungal pathogen affecting onion crops. The results from both seasons (Table 2 & 3) demonstrate that all zinc treatments, including both bulk ZnO and ZnO-Sca-NPs, significantly reduced the severity of downy mildew in onion compared to the untreated control, which consistently showed the highest disease severity at 63.47% and 57.03% in the first and second seasons, respectively. Fungicide treatment (Amistar top) was the most effective treatment across both seasons, recording the lowest disease severity (7.98and 10.12%) and the highest efficacy (87.43 and 82.25%). ZnO-Sca-NPs exhibited a clear dose-dependent response, with disease severity decreasing and efficacy increasing as

concentrations increased from 25 mg/L to 100 mg/L. ZnO-Sca-NPs NPs at 100 mg/L achieved 11.24 and 13.54% disease severity, with corresponding efficacy rates of 82.29 and 76.26% in the first and second seasons, respectively. Similarly, bulb yield improved significantly with ZnO-Sca-NPs NPs treatments, rising from 30.76 and 25.97 kg/plot at 25 mg/L to 39.68 and 36.87 kg/plot at 100 mg/L. Yield increases over the control ranged from 64.05–99.92% at 25 mg/L to 111.63–183.83% at 100 mg/L across the two seasons. Bulk ZnO also performed effectively, reducing disease severity to 16.01 and 15.34% in the first and second seasons, with efficacy values of 74.78 and 73.10%, respectively. Bulb yields under bulk ZnO reached 33.59 and 33.05 kg/plot, representing increases of 79.15 and 154.43% compared to the control. Although bulk ZnO was effective, ZnO-Sca-NPs at higher concentrations (75–100 mg/L) consistently outperformed it in both disease reduction and yield improvement.

Table 2. Effect of bulk zinc and ZnO-Sca-NPs treatments on disease severity of onion downy mildew and bulb yield under field conditions during the 2022-2023season.

Treatment	Disease severity Efficacy (%)		Bulb yield (Kg/plot)	Increases (%)	
ZnO-Sca-NPs 25mg/L	17.39 ^b	72.60	30.76 ^f	64.05	
ZnO-Sca-NPs 50 mg/L	15.78 ^{de}	75.14 31.98 ^b		70.56	
ZnO-Sca-NPs 75 mg/L	13.86 ^c	78.16	35.37 ^d	88.64	
ZnO-Sca-NPs 100 mg/L	11.24 ^d	82.29	39.68 ^c	111.63	
Bulk ZnO 2000mg/L	16.01 ^b	74.78	33.59 ^e	79.15	
Fungicide (Amistar top (SC) 300cm/feddan)	7.98 ^e	87.43	49.40 ^a	163.47	
Control without any treatments	63.47 ^a		18.75 ^g		
LSD at P value ≤ 0.05	2.03		1.67		

Different letters within each column indicate a significant difference according to the LSD test at P value \leq 0.05. P value at P value \leq 0.05 based on ANOVA followed by LSD test.

Table 3. Effect of bulk zinc and ZnO-Sca-NPs treatments on disease severity of onion downy mildew and bulb yield under field conditions during the 2023-2024 season.

Treatment	Disease severity	Efficacy (%)	Bulb yield (Kg/Plot)	Increases (%)
ZnO-Sca-NPs 25 mg/L	21.06 ^b	63.07	25.97 ^e	99.92
ZnO-Sca-NPs 50 mg/L	19.15 ^c	66.42	29.68 ^d	130.72
ZnO-Sca-NPs 75 mg/L	14.97 ^d	73.75	32.75 ^c	152.11
ZnO-Sca-NPs 100 mg/L	13.54d ^e	76.26	36.87 ^b	183.83
Bulk ZnO 2000mg/L	15.34 ^e	73.10	33.05 ^a	154.43
Fungicide (Amistar top (SC) 300cm/feddan)	10.12 ^f	82.25	40.23 ^a	209.70
Control without any treatments	57.03 ^a		12.99 ^f	
LSD at P value ≤ 0.05	2.15		1.82	

Different letters within each column indicate a significant difference according to the LSD test at P value \leq 0.05. P value at P value \leq 0.05 based on ANOVA followed by LSD test.

• Effect of bulk zinc and ZnO-Sca-NPs treatments on biochemical changes:

• Phenolic contents:

The data (Tables 4 & 5) from both seasons revealed that zinc treatments, whether in bulk form (ZnO) or as nanoparticles (ZnO-Sca-NPs) at four concentrations, significantly increased the phenolic content of onion plants compared to the untreated control. In the first season (2022-2023), the control plants showed the lowest levels of

total phenols (3.35 mg/g), conjugated phenols (2.11 mg/g), and free phenols (1.24 mg/g). In contrast, ZnO-Sca-NPs at 100 mg/L achieved the highest phenolic content, with 12.51 mg/g total phenols, 8.73 mg/g conjugated phenols, and 3.78 mg/g free phenols. A similar trend was observed in the second season, where ZnO-Sca-NPs NPs at 100 mg/L/Lproduced 13.64 mg/g total phenols, 9.81 mg/g conjugated phenols, and 3.83 mg/g free phenols, representing significant increases over the control (4.50, 3.13, and 1.37 mg/g, respectively). Dose-dependent effects were evident with ZnO-Sca-NPs across both seasons, as phenolic content increased progressively from 25 mg/L to 100 mg/L. Fungicide treatment also increased phenolic content compared to the control, with total phenols of 9.66 and 10.52 mg/g in the first and second seasons, respectively, although still lower than those obtained with ZnO-Sca-NPs at 75 and 100 mg/L.

Table 4. Effect of bulk zinc and ZnO-Sca-NPs treatments on phenolic content of onion plant infected with downy mildew under field conditions during the first growing season (2022-2023).

Treatment	Total phenols	Conjugated phenols	Free phenol	
ZnO-Sca-NPs 25mg/L	7.87 ^c	5.21 ^{cd}	2.66a ^b	
ZnO-Sca-NPs 50 mg/L	8.21 ^{bc}	4.99 ^d	3.22 ^a	
ZnO-Sca-NPs 75 mg/L	11.98 ^a	7.65a ^b	4.33 ^a	
ZnO-Sca-NPs 100 mg/L	12.51 ^a	8.73 ^a	3.78 ^a	
Bulk ZnO 2000 mg/L	8.73 ^{bc}	5.09 ^d	3.64 ^a	
Fungicide (Amistar top (SC) 300cm/feddan)	9.66 ^b	6.82 ^{bc}	2.84 ^{ab}	
Control without any treatments	3.35 ^d	2.11 ^e	1.24 ^b	
LSD at P value ≤ 0.05	0.94	0.88	0.76	

Different letters within each column indicate a significant difference according to the LSD test at P value \leq 0.05. P value at P value \leq 0.05 based on ANOVA followed by LSD test.

Table 5. Effect of bulk zinc and ZnO-Sca-NPs treatments on phenolic content of onion plant infected with downy mildew under field conditions during the second growing season (2023-2024).

Treatment	Total phenols	Conjugated phenols	Free phenol		
ZnO-Sca-NPs 25 mg/L	8.70 ^c	5.91 ^{cd}	2.79 ^{bc}		
ZnO-Sca-NPs 50 mg/L	9.74 ^{bc}	5.87 ^d	3.87 ^{ab}		
ZnO-Sca-NPs 75 mg/L	12.97 ^a	8.38 ^{ab}	4.59 ^a		
ZnO-Sca-NPs 100 mg/L	13.64 ^a	9.81 ^a	1 ^a 3.83 ^{ab}		
Bulk ZnO 2000mg/L	8.98 ^{bc}	5.57 ^d	3.41 ^{ab}		
Fungicide (Amistar top (SC) 300cm/feddan)	10.52 ^b	7.54 ^{bc}	2.98 ^{abc}		
Control without any treatments	4.50 ^d	3.13 ^e	1.37 ^c		
LSD at P value ≤ 0.05	1.12	0.94	0.85		

Different letters within each column indicate a significant difference according to the LSD test at P value \leq 0.05. P value at P value \leq 0.05 based on ANOVA followed by LSD test .SDS-PAGE Electrophoresis

SDS-PAGE analysis of total soluble proteins extracted from onion plants (Fig. 4, Table 6) revealed the presence of a distinct protein band (~48 kDa) in all treatments involving zinc-based zinc oxide (ZnO-Sca-NPs) nanoparticles, bulk ZnO, and the untreated control. The consistent appearance of this band across treatments indicates that both nano- and bulk-zinc applications are associated with the expression or accumulation of a specific protein potentially involved in the plant's response to downy mildew infection. Notably, the band intensity and lane percentage increased progressively with higher concentrations of ZnO-Sca-NPs, suggesting a dose-dependent enhancement in protein expression or stability. The highest band intensity (1,482,592) and lane percentage (7.814%) were recorded at 100 ppm ZnO-Sca-NPs NPs, followed by 75, 50, and 25 ppm treatments, respectively. This variation indicates that ZnO-Sca-NPs can stimulate the synthesis of the 48 kDa protein more effectively at elevated concentrations, possibly due to their greater surface area and reactivity. The relative mobility (Rf) values remained relatively constant (0.477–0.499), indicating no significant change in electrophoretic migration among treatments. Collectively, these findings suggest that ZnO-Sca-NPs modulate protein expression in

a concentration-dependent manner, potentially enhancing the activation of pathogenesis-related (PR) proteins and strengthening the onion plant's defense mechanisms against downy mildew infection.

Table 6. Protein band characteristics of onion treated with different concentrations of ZnO-Sca-NPs nanoparticles compared to the untreated control. Parameters include molecular weight (MW), band volume intensity, lane percentage, band width, and relative mobility (Rf).

Treatments	No. of Band	MW (KDa)	volume	Lane%	width	Rf
ZnO-Sca-NPs 25 mg/L	1	48	824699	4.204	52	0.492
ZnO-Sca-NPs 50 mg/L	1	48	1018699	5.764	71	0.480
ZnO-Sca-NPs 75 mg/L	1	48	1246798	6.539	77	0.480
ZnO-Sca-NPs 100 mg/L	1	48	1482592	7.814	84	0.499
Control without any treatments	1	48	741141	4.135	52	0.477
Bulk ZnO 2000mg/L	1	48	812439	4.039	51	0.489

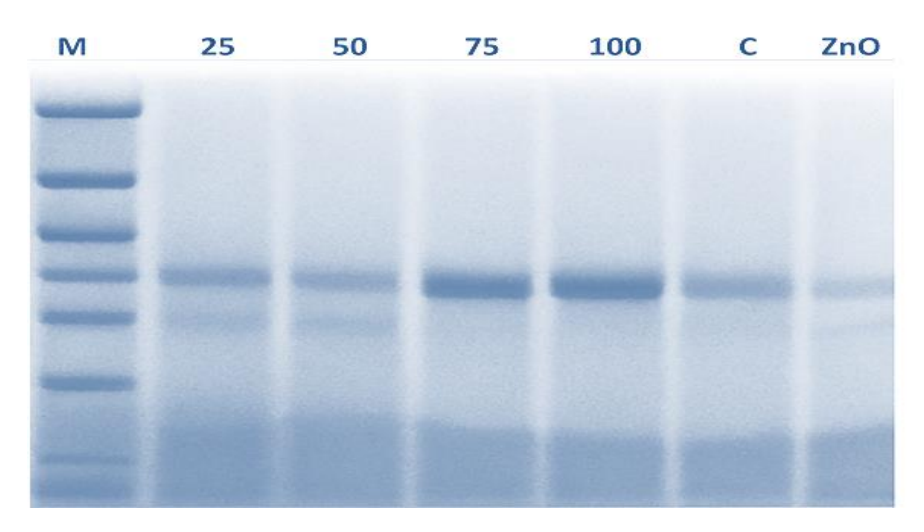


Fig. 4. SDS-PAGE protein expression profile from the onion plant treated with bulk zinc and ZnO-Sca-NPs.. A standard protein molecular weight marker can be seen in Lane M.

• Cytotoxic activity test of ZnO-Sca-NPs nanoparticles on normal human cells (Primary uterine fibroblast cells Line) using the MTT assay:

To evaluate the cytotoxic effect of ZnO-Sca-NPs nanoparticles on normal human cells (Primary uterine fibroblast cells Line) using the MTT assay at different time points (48 and 72 hours) at doses 25,50,75,100 mg/L to determine an appropriate dose (Table 7 & Fig. 5, 6).

The MTT assay results for normal human cells treated with ZnO-Sca-NPs nanoparticles over 48 and 72 hours indicate a significant time-dependent reduction in cell viability. A marked decrease in cell viability was observed over time, with higher viability at 24 hours compared to 72 hours.

No noticeable effect in cell viability was noted between the treatment groups at concentrations of 25-50mg/L, maintaining over 85% viability in these groups. The data also reveal that cell viability remained high at lower nanoparticle concentrations (25-50mg/L) even after 72 hours of exposure.

The IC_{50} value, which represents the concentration at which 50% of cells remained viable, decreased from 116.8 mg/L at 48 hours to 97.16 mg/L at 72 hours, indicating increased cytotoxicity with longer exposure durations.

Table 7. IC₅₀ of normal human cells (Primary uterine fibroblast cells Line) treated with ZnO-Sca-NPs nanoparticles, using the MTT assay at different time points (48 and 72 hours).

Sample Code	IC ₅₀ (mg/L)	
ZnO-Sca-NPs 48hr	116.8	
ZnO-Sca-NPs 72hr	97.16	

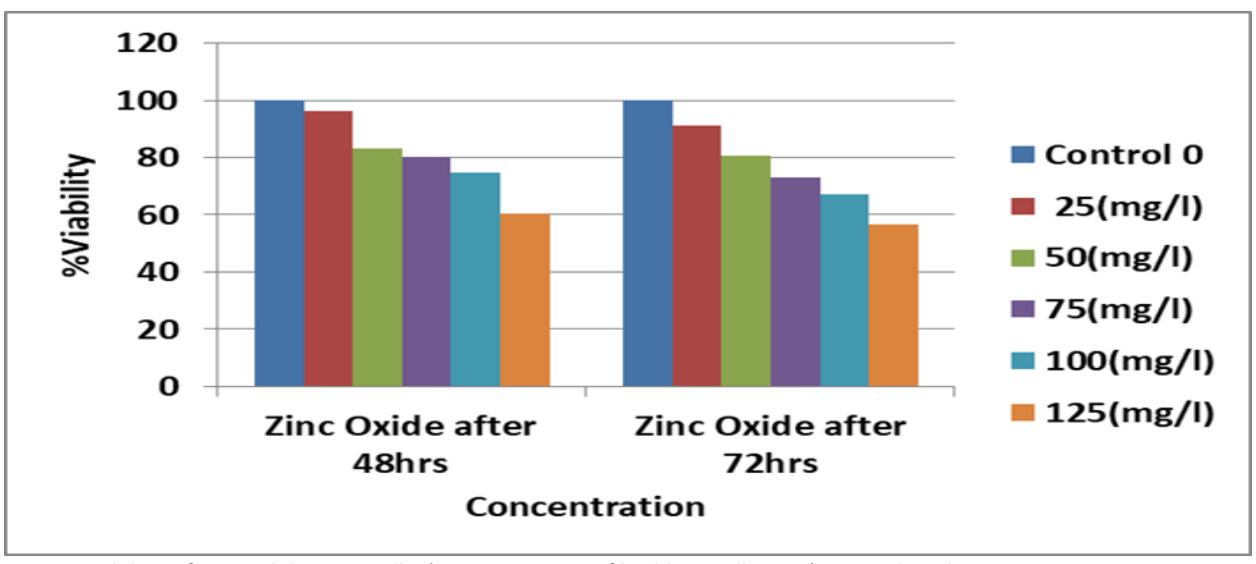


Fig. 5. Viability of normal human cells (Primary uterine fibroblast cells Line) treated with ZnO-Sca-NPs nanoparticles, using the MTT assay at different time points (48 and 72 hours).

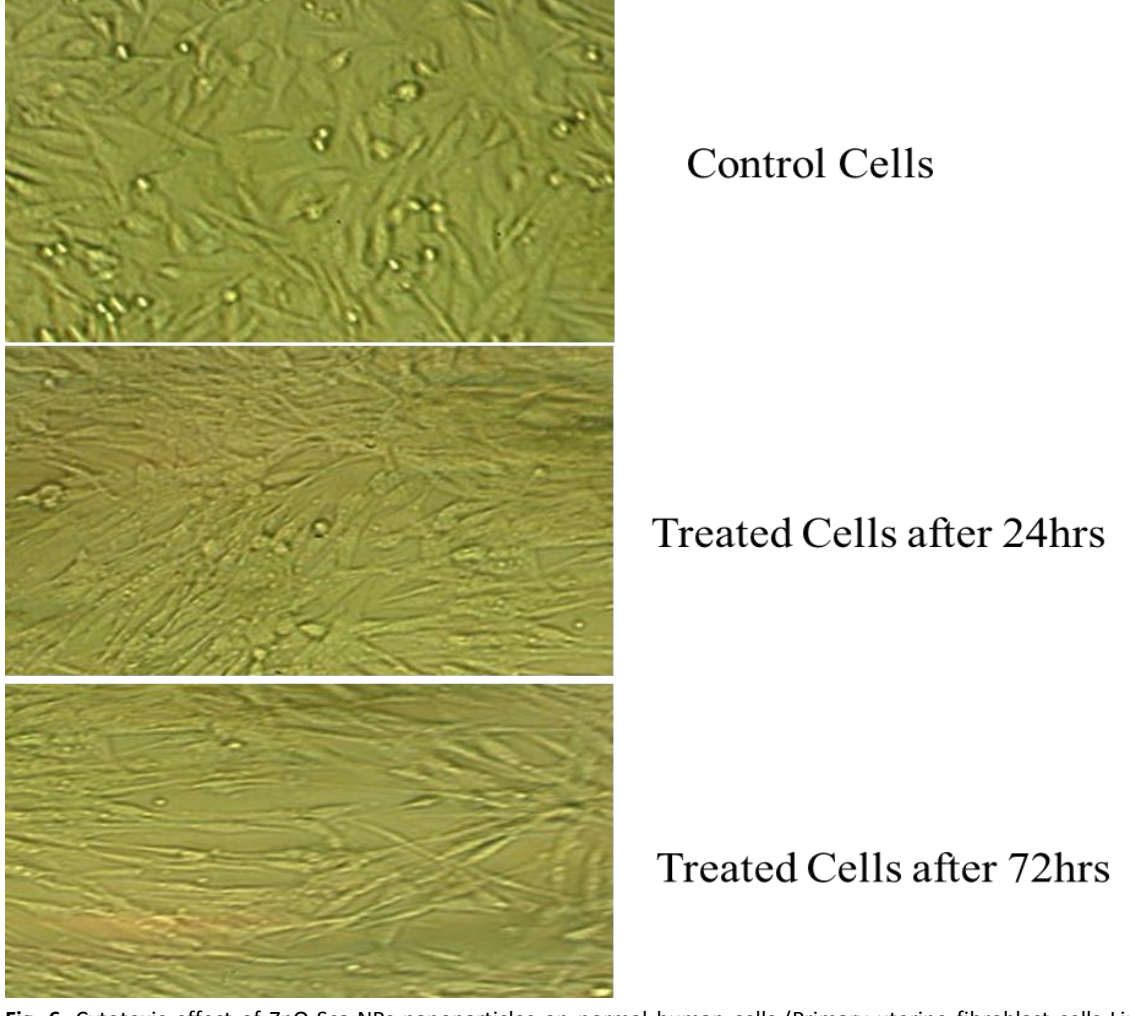


Fig. 6. Cytotoxic effect of ZnO-Sca-NPs nanoparticles on normal human cells (Primary uterine fibroblast cells Line) using the MTT assay at different time points (48 and 72 hours) at 100 mg/L. *Viability % = 100 x OD570t/OD570c.

DISCUSSION

A. cepa is an essential vegetable crop in Egypt, with onions ranking as the fourth largest export item. It is a dietary essential and possesses health-enhancing properties due to its many bioactive compounds. Onion is utilized in culinary processing, preservation, traditional medicine, and industrial applications. Nonetheless, it is sometimes affected by the oomycete disease P. destructor, which causes onion downy mildew. The disease develops in cold, humid conditions, resulting in considerable yield and bulb degradation. The disease has been progressively more widespread since 2016, presenting a significant risk to local production and export abilities. Current methods of management depend on fungicidal sprays; nevertheless, the rise of fungicide-resistant strains and environmental issues highlight the necessity for more effective and sustainable alternatives (Ahmed et al., 2021; Ministry of Agriculture and Land Reclamation, 2022). The diversity of bioactive compounds in plants continues to attract scientific interest due to their pharmacological properties, which mitigate the risk of disease (Naczk and Shahidi, 2006) and protect against oxidative stress by functioning as natural antioxidants (El-Abeid et al., 2024a). These beneficial effects are mainly attributed to secondary metabolites that play crucial roles in the plant life cycle, including pollinator attraction and defense against biotic and abiotic stressors (Vyavahare et al., 2025).

GC-MS analysis of S. arboricola extract identified thirteen major phytochemical constituents, primarily in the form of their trimethylsilyl (TMS) derivatives. Caffeic acid, a well-known hydroxycinnamic acid with antioxidant and anti-inflammatory properties (Chen and Ho, 1997), was the most dominant compound. Other prominent metabolites included malic acid, 4-coumaric acid, and arabino furanose. Minor constituents, such as ferulic acid, citric acid, palmitic acid, alpha-linolenic acid, and sebacic acid, may still exert synergistic effects that enhance antioxidant capacity, lipid metabolism, and plant defense (Wang et al., 2020; Rahim et al, 2023). Overall, this phytochemical profile highlights the potential of S. arboricola extract in pharmaceutical, nutraceutical, and plant biotechnology applications (Edo et al., 2025). In nanoparticle synthesis, the primary objective is to identify natural sources rich in bioactive molecules capable of serving as both reducing and stabilizing agents. This green approach promotes sustainability and minimizes toxicity compared to conventional chemical methods. In the present study, S. arboricola extract contained compounds such as caffeic acid, which played a pivotal role in the green synthesis of zinc nanoparticles (Choi et al., 2017). TEM analysis confirmed the formation of uniformly distributed spherical ZnO-Sca-NPs, demonstrating the extract's dual reducing and stabilizing function. These results are consistent with previous findings by (Choudhary et al., 2023), who attributed similar morphological characteristics to caffeic acidmediated synthesis mechanisms. Furthermore, the absorption band centered around 1567 cm⁻¹ corresponds to C=C stretching vibrations in aromatic rings. The peak at 1396 cm⁻¹ is associated with O-H bending in carboxylic acid groups, while the band near 1337 cm⁻¹ likely arises from O-H bending vibrations in alcohol groups. The FTIR spectra revealed prominent absorption bands in the range of 1567-1337 cm-1, corresponding to the asymmetric and symmetric stretching vibrations of the carboxylate (-COO) group. These spectral features align with the findings of (Choi et al., 2017), who demonstrated that caffeic acid can form covalent interactions with Zn²⁺ ions on the surfaces of ZnO nanoparticles (ZnONPs). The presence of characteristic functional groups (hydroxyl O-H, carbonyl C=O, and aromatic C=C further supports the involvement of phenolic and carboxylic moieties in metal ion chelation and nanoparticle stabilization. This suggests that caffeic acid plays a dual role in both binding Zn²⁺ ions and capping the nanoparticles. Additionally, XRD analysis confirmed the crystallinity of the synthesized ZnO-Sca-NPs, showing a welldefined hexagonal wurtzite structure with minimal impurity signals. These results highlight the effectiveness of S. arboricola extract as an eco-friendly, biogenic agent for the synthesis of highly crystalline and stable ZnO-Sca-NPs.

Zinc plays a vital role in plant physiology, contributing to reactive oxygen species (ROS) modulation, membrane stability, and the activation of pathogenesis-related (PR) proteins, which enhance disease tolerance (Rao *et al.*, 2025). The yield increase observed in ZnO-Sca-NPs -NP-treated plots reflects zinc's dual role in disease suppression and metabolic enhancement, participating in chlorophyll biosynthesis, auxin metabolism, and carbohydrate utilization (Suzan *et al.*, 2025). Although the fungicide treatment produced the highest yield (49.40 and 40.23 kg/plot across two seasons), the 100 mg/L ZnO-Sca-NPs showed comparable results with an ecofriendlier profile (Ong *et al.*, 2018; Iqbal *et al.*, 2022). A consistent dose-dependent trend was observed, where increasing ZnO-Sca-NPs concentration from 25 to 100 mg/L enhanced total and free phenolic contents, reflecting stronger biochemical responses to higher ZnO-NP availability. Wang *et al.*, (2023) similarly reported that ZnONPs induce systemic resistance via phenylalanine ammonia-lyase (PAL) activation. While fungicide treatment also elevated phenolic levels, they remained significantly lower than those induced by 100 mg/L ZnO-NPs (Cruz-Luna *et al.*, 2021). This suggests that ZnO-Sca-NPs act not only as nutrients but also as elicitors of plant defense, promoting

biochemical resilience against biotic stress. Protein expression patterns further supported this conclusion, showing dose-dependent induction associated with PR protein activation and enhanced immune responses (Kumar *et al.*, 2025). These findings align with previous research suggesting that nanomaterials, due to their high surface reactivity, can more effectively trigger defense mechanisms, providing an efficient strategy for controlling onion downy mildew (Jadoun *et al.*, 2021).

Cytotoxicity assessment using primary uterine fibroblast cells confirmed the relative safety of ZnO–Sca–NPs at low doses. These normal, non-transformed cells provide a physiologically relevant model for evaluating nanoparticle toxicity (Vivek and Kannan, 2012; Anjum *et al.*, 2021). Results showed no significant cytotoxic effect at 25–50 mg/L, as cell viability remained above 85% after 72 hours. However, higher concentrations caused notable declines in viability, indicating dose-dependent toxicity (Ng *et al.*, 2017; Pinho *et al.*, 2020; Xuan *et al.*, 2023; Al-Momani *et al.*, 2024). This suggests that ZnO–Sca–NPs are biocompatible at low levels but require careful dose optimization for biomedical applications (Abd-Elmaqsoud *et al.*, 2022). The superior disease suppression achieved by ZnO–Sca–NPs compared with bulk ZnO and ZnSO₄ treatments can be attributed to improved zinc bioavailability and nanoscale properties enhancing plant uptake and systemic activity (Rizwan *et al.*, 2019; Singh *et al.*, 2021). The 100 mg/L concentration provided optimal disease reduction without phytotoxicity, confirming its efficiency as a sustainable alternative to chemical fungicides. The improved onion growth and yield following ZnO–Sca–NP application may result from enhanced nutrient absorption, chlorophyll biosynthesis, and carbohydrate partitioning (Alloway, 2008; Faizan *et al.*, 2018; Abd El-Latef *et al.*, 2023).

The observed increases in protein, and antioxidant enzyme activities (POD and PPO) in ZnO–Sca–NP-treated plants reflect improved zinc-mediated enzymatic activity and induced defense mechanisms. These biochemical enhancements strengthen the plant's tolerance to oxidative and pathogen stress, supporting previous observations (Rizwan et al., 2019; Choudhary et al., 2023). The biogenic capping by Schefflera extract may further enhance nanoparticle stability and controlled nutrient release, contributing to superior performance compared with non-biogenic zinc treatments. Overall, ZnO–Sca–NPs act as both nutrient and biostimulant agents, promoting photosynthetic efficiency, enzymatic defense, and yield enhancement in an environmentally sustainable manner. Finally, integrating sustainability assessment using the Need–Quality–Sustainability (NQS) Index provides a valuable framework for evaluating green nanotechnology approaches (Saleh et al., 2025a,b). This concept aligns with multiple United Nations Sustainable Development Goals (SDGs). Green-synthesized nanoparticles contribute to SDG 3 (Good Health and Well-Being) through safer biomedical and agricultural applications, SDG 12 (Responsible Consumption and Production) by minimizing hazardous reagents and waste, and SDG 17 (Partnerships for the Goals) by promoting interdisciplinary collaborations (Mohamed et al., 2023; El-Abeid et al., 2024b; Harb et al., 2024). Collectively, these outcomes demonstrate that Schefflera-mediated ZnO nanoparticles represent a promising, sustainable, and multifunctional platform for both agricultural and biomedical applications.

CONCLUSION

This study demonstrated the green synthesis of ZnONPs using *S. arboricola* extract. The nanoparticles effectively reduced the severity of onion downy mildew, enhanced bulb yield, and increased phenolic content, with activation of a ~48 kDa defense-related protein. Cytotoxicity tests confirmed good biocompatibility at low concentrations. Overall, ZnO-Sca-NPs represent a safe, eco-friendly alternative to conventional fungicides, promoting sustainable crop protection and growth enhancement.

REFERENCES

- Abd El-Latef, E. A., Wahba, M. N., Mousa, S., El-Bassyouni, G. T., & El-Shamy, A. M. (2023). Cu-doped ZnO-nanoparticles as a novel eco-friendly insecticide for controlling *Spodoptera littoralis*. *Biocatalysis and Agricultural Biotechnology*, *52*, 102823.
- Abd El-Fattah, N. G., Abd El-Baki, M. S., Ibrahim, M. M., Sharaf-Eldin, M., & Elsayed, S. (2024). Evaluating the performance of data-driven models combined with IoT to predict the onion yield under different irrigation regimes. *Egyptian Journal of Soil Science*, 64(4), 1549–1566.
- Abd-Elmaqsoud, I. G., Elsaadawi, H. A., Ahmed, A. I., AbdelKhalek, A., & Arisha, A. H. (2022). The vast biomedical applications of zinc oxide nanoparticles. *Zagazig Veterinary Journal*, 50(3), 107–115.
- Agricultural Economics Research Institute. (2023). Commodity reports series: Onion crop. Agricultural Research Center.
- Ahmed, Y. A., Ismail, A. E., & Mansour, M. T. (2021). Evaluation of fungicide resistance in Peronospora destructor

- populations from onion fields in Egypt. Egyptian Journal of Plant Pathology, 49(2), 145-158.
- Alloway, B. J. (2008). Zinc in soils and crop nutrition. Second edition, published by IZA and IFA Brussels, Belgium and Paris, France, 136 PP.
- Al-Momani, H., Aolymat, I., Ibrahim, L., Albalawi, H., Al Balawi, D. A., Albiss, B. A., ... & Alghweiri, S. (2024). Low-dose zinc oxide nanoparticles trigger the growth and biofilm formation of Pseudomonas aeruginosa: a hormetic response. *BMC microbiology*, *24*(1), 290.
- Gupta, A. J., Kaldate, S., Volaguthala, S., & Mahajan, V. (2025). Onion nutritional and nutraceutical composition and therapeutic potential of its phytochemicals assessed through preclinical and clinical studies. *Journal of Functional Foods*, 129, 106889.
- Amr, S. S. S., & Darwish, M. A. M. (2019). An economic study of onion and garlic crops in Fayoum Governorate. Egyptian Journal of Agricultural Economics, 29(4B), [December Issue].
- Anjum, S., Hashim, M., Malik, S. A., Khan, M., Lorenzo, J. M., Abbasi, B. H., & Hano, C. (2021). Recent advances in zinc oxide nanoparticles (ZnO NPs) for cancer diagnosis, target drug delivery, and treatment. *Cancers*, *13*(18), 4570.
- Bradford, M. M. (1976). A rapid and sensitive method for the quantitation of microgram quantities of protein utilizing the principle of protein-dye binding. *Analytical Biochemistry*, 72(1-2), 248-254.
- Chen, J. H., & Ho, C. T. (1997). Antioxidant activities of caffeic acid and its related hydroxycinnamic acid compounds. *Journal of Agricultural and Food Chemistry*, 45(7), 2374-2378.
- Chinnasami, S., & Manickam, R. (2023). Classification of the architecture using IBM SPSS statistics. REST Publisher.
- Choi, K. H., Nam, K. C., Lee, S. Y., Cho, G., Jung, J. S., Kim, H. J., & Park, B. J. (2017). Antioxidant potential and antibacterial efficiency of caffeic acid-functionalized ZnO nanoparticles. *Nanomaterials*, 7(6), 148.
- Choudhary, S., Sharma, R., Devi, A., Thakur, A., Giri, S. K., Nagar, S., & Singh, G. (2023). Green synthesis of copper nanoparticles and their evaluation for antimicrobial activity and bio-compatibility. *Materials Today: Proceedings*.
- Cruz-Luna, A. R., Cruz-Martínez, H., Vásquez-López, A., & Medina, D. I. (2021). Metal nanoparticles as novel antifungal agents for sustainable agriculture: Current advances and future directions. *Journal of Fungi*, 7(12), 1033.
- Drishya, P. K., Reddy, M. V., Mohanakrishna, G., Sarkar, O., Isha, Rohit, M. V., ... & Chang, Y. C. (2025). Advances in microbial and plant-based biopolymers: synthesis and applications in next-generation materials. *Macromol*, *5*(2), 21.
- Edo, G. I., Mafe, A. N., Ali, A. B., Akpoghelie, P. O., Yousif, E., Isoje, E. F., ... & Alamiery, A. A. (2025). Green biosynthesis of nanoparticles using plant extracts: mechanisms, advances, challenges, and applications. *Bio Nano Science*, *15*(2), 267.
- El-Abeid, S. E., Ansari, R. A., Mosa, M. A., Soliman, A. G., Saleh, A. M., Boudaden, J., & Ibrahim, D. S. (2024). Nanosensors: An emerging tool for early detection of plant pathogens in sustainable agriculture. In *Nanotechnology and Plant Disease Management* (pp. 61-70). CRC Press.
- El-Abeid, S. E., Mosa, M. A., El-Tabakh, M. A., Saleh, A. M., El-Khateeb, M. A., & Haridy, M. S. (2024a). Antifungal activity of copper oxide nanoparticles derived from *Zizyphus spina* leaf extract against Fusarium root rot disease in tomato plants. *Journal of Nanobiotechnology*, 22(1), 28.
- Faizan, M., Faraz, A., Yusuf, M., Khan, S. T., & Hayat, S. (2018). Zinc oxide nanoparticle-mediated changes in photosynthetic efficiency and antioxidant system of tomato plants. *Photosynthetica*, *56*(2), 678-686.
- FAO (Food and Agriculture Organization of the United Nations) (2023). (n.d.). Official website. http://www.fao.org Galván, G. A., Tikunov, Y., Bovy, A., de Vos, R., & Lindhout, P. (2008). Downy mildew resistance in onion: Physiology and molecular perspectives. *Euphytica*, 159(1–2), 135–145.
- Guseva, N. N., & Gromova, B. B. (1982). Chemical and biochemical methods for studying plant immunity. *All Union Institute of Plant Protection, Leningrad, USSR*.
- Harb, H. E., El-Tabakh, M. A., Khattab, A. M., Mohamed, Y. A., Saleh, A. M., & El-Abeid, S. E. (2024). Recent advances of using innovative strategies in management of millet plant pathogens. *Genetic Improvement of Small Millets*, 297-328.
- Iqbal, Z., Tanweer, M. S., & Alam, M. (2022). Recent advances in adsorptive removal of wastewater pollutants by chemically modified metal oxides: A review. *Journal of Water Process Engineering*, 46, 102641.
- Jadoun, S., Arif, R., Jangid, N. K., & Meena, R. K. (2021). Green synthesis of nanoparticles using plant extracts: A review. *Environmental Chemistry Letters*, *19*(1), 355-374.

- Koike, S. T., Gladders, P., & Paulus, A. O. (2007). *Vegetable diseases: a color handbook*. Gulf Professional Publishing. Kumar, P., Pandey, S., & Pati, P. K. (2025). Interaction between pathogenesis-related (PR) proteins and phytohormone signaling pathways in conferring disease tolerance in plants. *Physiologia Plantarum*, 177(2),
 - e70174.
- Laemmli, U. K. (1970). Cleavage of structural proteins during the assembly of the head of bacteriophage T4. *Nature*, 227(5259), 680-685.
- Mahmoud, E. E. D., Hussien, Z., Ibrahim, M., & Abdel-Gayed, M. (2016). Compatibility between chemical inducers and Amistar top fungicide for controlling onion downy mildew and purple blotch diseases. *Egyptian Journal of Phytopathology*, 44(2), 67-84.
- Ministry of Agriculture and Land Reclamation. (2022). Agricultural statistical bulletins. *Central Administration of Agricultural Economics*.
- Ministry of Agriculture and Land Reclamation. (2023). Annual report on onion diseases in Egypt.
- Mohamed Saleh, A., El-Kosasy, A. M., & Fares, N. V. (2023). UV Spectrophotometric Method Development and validation of vonoprazan fumarate in Bulk and pharmaceutical Dosage form; Green Profile Evaluation Via eco-scale And GAPI Tools. *Egyptian Journal of Chemistry*, 66(8), 141-148.
- Naczk, M., & Shahidi, F. (2006). Phenolics in cereals, fruits and vegetables: Occurrence, extraction and analysis. *Journal of Pharmaceutical and Biomedical Analysis*, 41(5), 1523-1542.
- Ng, C. T., Yong, L. Q., Hande, M. P., Ong, C. N., Yu, L. E., Bay, B. H., & Baeg, G. H. (2017). Zinc oxide nanoparticles exhibit cytotoxicity and genotoxicity through oxidative stress responses in human lung fibroblasts and Drosophila melanogaster. *International Journal of Nanomedicine*, 1621-1637.
- Nicastro, H. L., Ross, S. A., & Milner, J. A. (2015). Garlic and onions: their cancer prevention properties. *Cancer Prevention Research*, 8(3), 181-189.
- Ong, C. B., Ng, L. Y., & Mohammad, A. W. (2018). A review of ZnO nanoparticles as solar photocatalysts: Synthesis, mechanisms and applications. *Renewable and Sustainable Energy Reviews*, 81, 536-551.
- Pinho, A. R., Martins, F., Costa, M. E. V., Senos, A. M., da Cruz e Silva, O. A., Pereira, M. D. L., & Rebelo, S. (2020). In vitro cytotoxicity effects of zinc oxide nanoparticles on spermatogonia cells. *Cells*, *9*(5), 1081.
- Raghupathi, K. R., Koodali, R. T., & Manna, A. C. (2011). Size-dependent bacterial growth inhibition and mechanism of antibacterial activity of zinc oxide nanoparticles. *Langmuir*, *27*(7), 4020-4028
- Raha, S., & Ahmaruzzaman, M. (2022). ZnO nanostructured materials and their potential applications: progress, challenges and perspectives. *Nanoscale Advances*, *4*(8), 1868-1925.
- Rahim, M. A., Ayub, H., Sehrish, A., Ambreen, S., Khan, F. A., Itrat, N., ... & Rocha, J. M. (2023). Essential components from plant source oils: a review on extraction, detection, identification, *and quantification*. *Molecules*, 28(19), 6881.
- Rao, M. J., Duan, M., Zhou, C., Jiao, J., Cheng, P., Yang, L., ... & Zheng, B. (2025). Antioxidant defense system in plants: Reactive oxygen species production, signaling, and scavenging during abiotic stress-induced oxidative damage. *Horticulturae*, *11*(5), 477.
- Rizwan, M., Ali, S., Ali, B., Adrees, M., Arshad, M., Hussain, A., ... & Waris, A. A. (2019). Zinc and iron oxide nanoparticles improved the plant growth and reduced the oxidative stress and cadmium concentration in wheat. *Chemosphere*, 214, 269-277.
- Sagar Raut, D. P., & Thorat, R. (2015). Green synthesis of zinc oxide (ZnO) nanoparticles using *Ocimum tenuiflorum* leaves. *International Journal of Scientific Research*, 4(5), 1225-1228.
- Saleh, A. M., Hassan, R. Y., Badawey, A. M., & Marzouk, H. M. (2025). Software-assisted evaluation of sustainable chemistry innovations: A critical analytical review of viability assays incorporating diseases' biomarkers with greenness, blueness, and whiteness computational metrics. *Microchemical Journal*, 114437.
- Saleh, A. M., Saleh, O. A., Hassan, R. Y., Badawey, A. M., & Marzouk, H. M. (2025). A novel quality-by-design assisted HPLC-DAD method for the simultaneous quantification of tryptophan, tryptophol, and voriconazole for early diagnosis and prognosis of fungal infections decoding quorum sensing phenomenon. *Journal of Chromatography B*, 1257, 124571.
- Sammons, D. W., Adams, L. D., & Nishizawa, E. E. (1981). Ultrasensitive silver-based color staining of polypeptides in polyacrylamide gels. *Electrophoresis*, *2*(3), 135-141.
- Sangeeta, M. K., Tejashree, Gunagambhire, V. M., Bhat, M. P., Nagaraja, S. K., Gunagambhire, P. V., ... & Mahalingam, S. M. (2024). In-vitro evaluation of *Talaromyces islandicus* mediated zinc oxide nanoparticles for antibacterial, anti-inflammatory, bio-pesticidal and seed growth promoting activities. *Waste and*

- *Biomass Valorization, 15*(3), 1901-1915.
- Schwartz, H. F., & Mohan, S. K. (2007). Compendium of onion and garlic diseases and pests.
- Sethi, G., Behera, K. K., Sayyed, R., Adarsh, V., Sipra, B. S., Singh, L., ... & Behera, M. (2025). Enhancing soil health and crop productivity: the role of zinc-solubilizing bacteria in sustainable agriculture. *Plant Growth Regulation*, 1-17.
- Singh, P., Kim, Y. J., Zhang, D., & Yang, D. C. (2016). Biological synthesis of nanoparticles from plants and microorganisms. *Trends in Biotechnology*, *34*(7), 588-599.
- Singh, K., Madhusudanan, M., Verma, A. K., Kumar, C., & Ramawat, N. (2021). Engineered zinc oxide nanoparticles: an alternative to conventional zinc sulphate in neutral and alkaline soils for sustainable wheat production. *3 Biotech*, *11*(7), 322
- Sirelkhatim, A., Mahmud, S., Seeni, A., Kaus, N. H. M., Ann, L. C., Bakhori, S. K. M., ... & Mohamad, D. (2015). Review on zinc oxide nanoparticles: antibacterial activity and toxicity mechanism. *Nano-micro letters*, 7(3), 219-242.
- Sneath, P. H., & Sokal, R. R. (1973). Numeral taxonomy. WH: Freemam, San Francisco, California.
- Subbaiah, L. V., Prasad, T. N. V. K. V., Krishna, T. G., Sudhakar, P., Reddy, B. R., & Pradeep, T. (2016). Novel effects of nanoparticulate delivery of zinc on growth, productivity, and zinc biofortification in maize (*Zea mays* L.). *Journal of Agricultural and Food Chemistry*, 64(19), 3778-3788.
- Tammam, S. A., Farghali, K. A., & Majrashi, D. M. (2025). Potential effect of zinc application on chlorophyll stability and metabolic status in *Moringa oleifera* Lam. under salinity stress conditions. *Egyptian Journal of Botany*, 65(3), 73-81.
- Swain, M., Mishra, D., & Sahoo, G. (2025). A review on green synthesis of ZnO nanoparticles. *Discover Applied Sciences*, 7(9), 997.
- Terpiłowska, S., Siwicka-Gieroba, D., & Siwicki, A. K. (2018). Cell viability in normal fibroblasts and liver cancer cells after treatment with iron (III), nickel (II), and their mixture. *Journal of Veterinary Research*, 62(4), 535
- Thomas, C. E., Duthie, J. A., & Saxton, A. M. (2014). Epidemiology of downy mildew in onion: A review. *Plant Disease*, 98(5), 565–574.
- Townsend, G.R. and Heuberger J.W. 1943. Methods for estimating losses caused by disease in fungicide experiments. *Platelet Disorder Reporter*, 27(17), 340-343.
- Vivek, R., Thangam, R., Muthuchelian, K., Gunasekaran, P., Kaveri, K., & Kannan, S. (2012). Green biosynthesis of silver nanoparticles from *Annona squamosa* leaf extract and its in vitro cytotoxic effect on MCF-7 cells. *Process Biochemistry*, 47(12), 2405-2410.
- Vyavahare, G. D., Patil, R. R., & Park, J. H. (2025). Nanoparticle-assisted elicitation of therapeutically important secondary metabolites in plants. *Plant Growth Regulation*, 1-28.
- Wang, Y., Chen, X., Huang, Z., Chen, D., Yu, B., Yu, J., ... & Zheng, P. (2020). Dietary ferulic acid supplementation improves antioxidant capacity and lipid metabolism in weaned piglets. *Nutrients*, 12(12), 3811
- Wang, Z., Wang, S., Ma, T., Liang, Y., Huo, Z., & Yang, F. (2023). Synthesis of zinc oxide nanoparticles and their applications in enhancing plant stress resistance: A review. *Agronomy*, *13*(12), 3060
- Xuan, L., Ju, Z., Skonieczna, M., Zhou, P. K., & Huang, R. (2023). Nanoparticles-induced potential toxicity on human health: applications, toxicity mechanisms, and evaluation models. *MedComm*, *4*(4), e327
- Zieslin, N., & Ben-Zaken, R. J. P. P. (1993). Peroxidase activity and presence of phenolic substances in peduncles of rose flowers. *Plant physiology and Biochemistry (Paris)*, 31(3), 333-339



Copyright: © 2025 by the authors. Licensee EJAR, EKB, Egypt. EJAR offers immediate open access to its material on the grounds that making research accessible freely to the public facilitates a more global knowledge exchange. Users can read, download, copy, distribute, print or share a link to the complete text of the application under Creative Commons BY-NC-SA International License.

